ORIGINAL PAPER

The effects of ultrasound on the direct electrosynthesis of solid K$_2$FeO$_4$ and the anodic behaviors of Fe in 14 M KOH solution

Zhihua Xu · Jianming Wang · Wenqu Mao · Weichun He · Quanqi Chen · Jianqing Zhang

Abstract The effects of ultrasound on the direct electrosynthesis of solid K$_2$FeO$_4$ and the anodic behaviors of pure iron were investigated, and the physical properties of samples were characterized by means of X-ray diffraction, Fourier transform infrared spectroscopy, and scanning electron microscopy. The experimental results showed that the existence of ultrasound can decrease the formation potential of ferrate(VI) and the passivation extent of iron anode, and this leads to higher current efficiency for the direct electrosynthesis of solid ferrate(VI) at 65 °C in 14 M KOH solution. It was also found that, in the experimental scope suitable ultrasonic power (14.6 W), shorter electrolysis duration and smaller electrolysis current can improve the apparent current efficiency of the electrosynthesis, and the largest current efficiency under suitable experimental conditions reached 77.2%.

Keywords K$_2$FeO$_4$ · Ultrasound · Electrosynthesis · Pure iron · Efficiency

Introduction

Ferrate(VI) has gained increasing attention as an environmentally friendly oxidant applied in water treatment [1] and organic synthesis [2] as a safer alternative to other toxic oxidizing compounds such as chlorine and CrO$_3$, etc.

Z. Xu · J. Wang (✉) · W. Mao · W. He · Q. Chen · J. Zhang
Department of Chemistry, Zhejiang University,
Hangzhou 310027, People's Republic of China
e-mail: wjm@cmsce.zju.edu.cn

J. Zhang
Chinese State Key Laboratory for Corrosion and Protection,
Shenyang 110015, People's Republic of China

Ferrate(VI) has also been recently considered to be a promising cathode in super-iron batteries [3–9] due to its relatively high redox potential, large electrochemical capacity, and non-toxic discharge product.

Because of the above-mentioned potential applications, the preparation of ferrate(VI) has gained much attention [10–16]. Three methods have been used for preparation of ferrate(VI) [17], that is, (1) wet oxidation method, (2) dry oxidation method, and (3) electrochemical method. Electrochemical preparation has been developed quickly and widely in the recent years as no hazardous chlorinated compounds or/and other strong oxidants such as ozone are necessary, and the electrosynthesis process of K$_2$FeO$_4$ is relatively easy to operate. Unfortunately, the electrochemical method suffers from a much lower apparent current efficiency of ferrate(VI) production, which is considered to be due to the deactivation of the anode, by-product of O$_2$, and its decomposition in the electrolyte. To maintain a high ferrate(VI) generation yield over a long period and to rapidly generate high concentration of ferrate(VI), several modifications have been proposed to use for this purpose such as current reversal [10], a.c. modulation of the current [11, 12], a three-dimensional anode made from porous iron wool [14], a porous powder electrode [15], and direct preparation of solid potassium ferrate(VI) to minimize its decomposition in the electrolyte [13, 16]. However, to our knowledge, the effects of ultrasound on the electrosynthesis of K$_2$FeO$_4$ have not been reported in previous literatures, although the electrochemical behaviors of iron anode in the presence of ultrasound in acid solution were studied [18–20].

Ultrasound is well known for (1) enhancement of mass transfer in electrochemical process, (2) alteration of absorption and surface properties of the electrode, and (3) affecting the formation of solid products on the electrode surface, which results from cavitation and micro-

streaming [21, 22]. Numerous attractive applications, such as electrodeposition [23], electrosynthesis [24], and metal corrosion [25], actually result from the combination of ultrasound and electrochemistry.

In this paper, the effects of ultrasound on the direct electrosynthesis of solid K_2FeO_4 and the anodic behaviors of pure iron in 14 M KOH solution have been investigated for the first time.

Experimental

An electrolysis cell was made of poly(methyl methacrylate), including one anode chamber and two cathode chambers. The dimensions of the anode chamber and two cathode ones were 90×100×20 mm and 90×100×40 mm, respectively. The anode with a surface area of 548 cm^2 was made from commercial iron wire gauze covered with zinc layer, whose compositions and features had been previously described [16]. The cathodes were two pieces of nickel foam electrodes and the membrane between anode and cathode chambers was a common Nafion-like cationic exchange membrane with a thickness of 0.5 mm. The electrolyte was 14 M KOH, which was prepared from analytical-grade reagents and deionized water. Electrolysis cell temperature was carefully controlled by a large water bath with a cooling/heating control. Galvanostatic electrolysis was controlled by a Potentiostat/Galvanostat model WWL-3DL Power sources (Yangzhou Shuanghong Electronic, People's Republic of China). Before electrolysis, the anode was put in the concentrated alkaline solution for 1 h to remove the Zn layer then washed with deionized water carefully and dried in hot air. After electrolysis, 20~25 ml 3 M KOH chilled solution was used to dissolve the K_2FeO_4 adhered on the anode gauze and electrolysis cell and then added to 90 ml of the anolyte containing K_2FeO_4 at ~0 °C (using an ice bath). After stirring for 5 min, the mixture obtained was filtered on a Buchner, sintered glass filter and then washed three times with 60 ml of cyclohexane, followed by washing six times with 100 ml of chilled ethanol. The K_2FeO_4 powder was dried under vacuum (at 2~3 mbar), at about 80 °C for 2 h, yielding 3~5 g K_2FeO_4, and the purity was determined by chromite analysis [26].

The electrochemical tests were performed with a Potentiostat/Galvanostat (Model 273A from EG&G Princeton Applied Research). Before scanning electron microscopy (SEM) characterization for the pure iron anode, the electrolysis was carried out with ZF-8 Potentiostat/Galvanostat (Shanghai Zhengfang Electronic Apparatus, People's Republic of China). In these measurements, a conventional three-electrode glass cell was used. The working electrode was pure iron electrode (99.99%, Alfa Aesar) with surface area of 0.3165 cm^2 and Pt foil was used as a counter electrode in addition to a Hg/HgO in 14 M KOH solution reference electrode. In the presence of ultrasound, the reference electrode was outside the ultrasonic field.

Before each electrochemical test, pure iron electrode was polished by 2,000 grit waterproof abrasive paper, rinsed in deionized water, and cathodically polarized at −1.3 V for 10 min to obtain a reproducible surface.

The decomposition test of ferrate(VI) was performed in a 150-ml glass conical beaker. In each test, 10 ml 14 M KOH solution was added to the glass beaker, then 0.11 g potassium ferrate was put into the solution. After the glass beaker had been held in water bath or ultrasonic bath at 65 °C for 2 h, the ferrate(VI) content left was determined by chromite analysis.

The morphologies of samples were observed using a SEM with a SIRION microscopy (FEI, USA). X-ray diffraction (XRD) was tested using Rigaku D/Max 2550 X-ray diffractometer, with CuKα radiation at 40 kV and 300 mA, scan rate 8 ° (2θ)/min. Fourier transform infrared (FTIR) was measured using Nicolet Nexus 670 Fourier transform infrared.

Under ultrasonic conditions, the electrochemical cell was immersed into an ultrasonic bath. The ultrasonicator used was a KQ-50DB digital ultrasonic and cleaning reactor (Kunshan Ultrasonic Instrument, People's Republic of China). Stirring conditions were modified by changing the ultrasonic power at a nominal constant wave frequency of 40 kHz, and ultrasonic powers were determined calorimetrically [27, 28]. It should be noticed that more precise results may be obtained by ultrasonic probe systems with directed sound emission [29].

Results and discussion

Effects of ultrasound on the direct electrosynthesis of solid K_2FeO_4

Figure 1 illustrates the effects of ultrasonic power on the direct electrosynthesis of solid ferrate(VI) at 65 °C in 14 M KOH solution in terms of apparent current efficiency, purity, and yield. It can be seen that the ferrate(VI) electrosynthesis with ultrasound has higher current efficiency than that without ultrasound, and ultrasound produces little impact on the purity and yield of solid ferrate(VI). The highest current efficiency (71% for 2 h electrolysis) is obtained at 14.6 W ultrasonic power, which is about 16% larger than that without ultrasound. The existence of ultrasound can enhance the mass transfer and improve the surface state of the iron wire anode, thus the electrosynthesis of solid ferrate(VI) with ultrasound is improved in terms of current efficiency. However, as it is shown in Fig. 2, the decomposition amount of ferrate(VI)
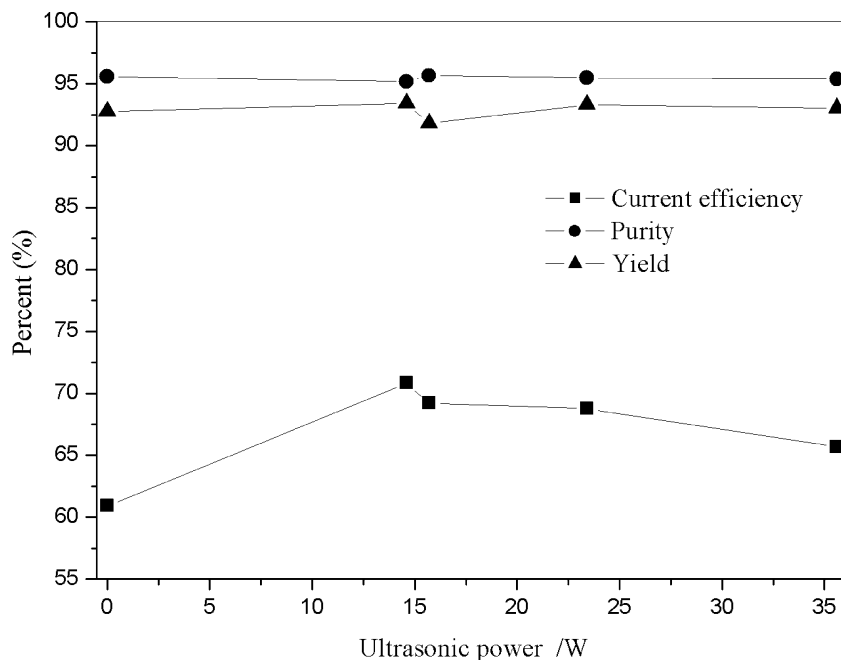
Fig. 1 Dependence of K$_2$FeO$_4$ electrosynthesis on ultrasonic power at 65°C in 14 M KOH. Duration of electrolysis, 2 h; current density, 2.74 mA cm^{-2} (I = 1,500 mA, $S_{(iron)}$= 548 cm^2); anode, iron wire gauze

under the same experimental conditions increases with the increase of ultrasonic power. This may be the reason why the apparent current efficiency slightly decreases with increasing ultrasonic power from 14.6 to 35.6 W.

Figure 3 probes the effects of electrolysis time on the apparent current efficiency, purity, and yield of solid K$_2$FeO$_4$ with and without 14.6 W ultrasound at 65 °C. In the presence of ultrasound, the highest apparent current efficiency 74.8% is obtained after 1 h electrolysis, and the

efficiency drops to ca. 71% for 2 h electrolysis, then it almost keeps unchanged from 2 to 4 h electrolysis duration. It is noted that the current efficiency has a relatively larger decrease in the fifth hour electrolysis duration. In the absence of ultrasound, the yield and purity of solid K$_2$FeO$_4$ are almost identical with those in the presence of ultrasound, and the current efficiency is much lower than that with ultrasound during the whole electrolysis duration, but it also has a decreasing trend with the increase of
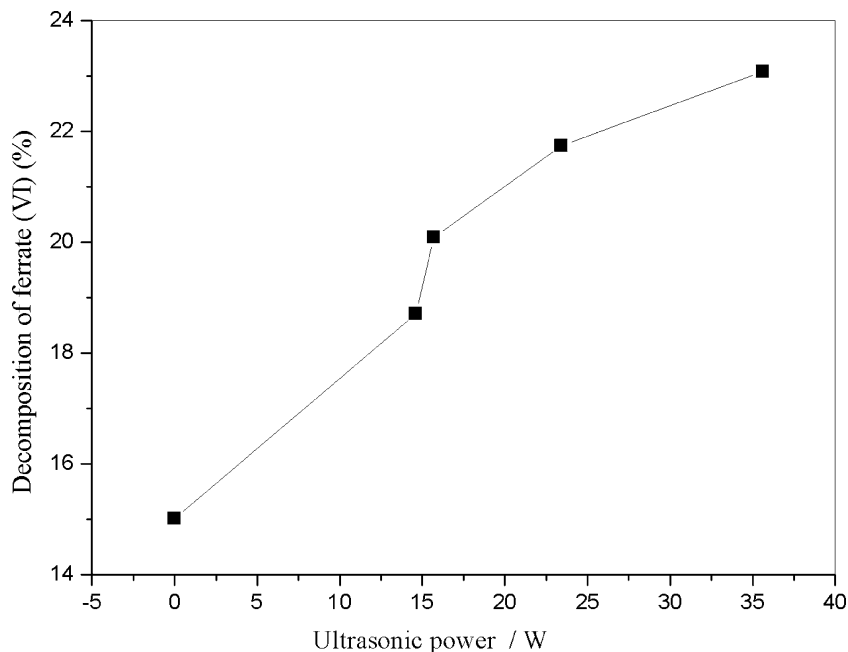

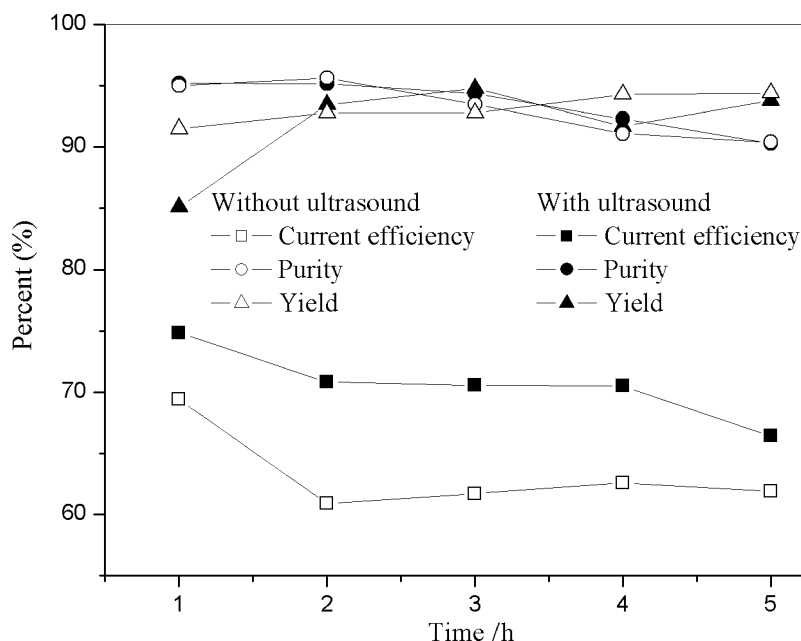**Fig. 2** Influence of ultrasonic power on the decomposition of K$_2$FeO$_4$ in 14 M KOH at 65 °C

Fig. 3 Dependence of K$_2$FeO$_4$ synthesis on electrolysis duration in 14 M KOH at 65 °C. Ultrasonic power, 14.6 W. Cell conditions are as described in Fig. 1 caption

electrolysis time. Higher apparent current efficiency for the direct electrosynthesis of solid ferrate(VI) with ultrasound might result from the continual activation of the anode surface, the improvement of solid ferrate(VI) transfer from the anode surface, and/or lower O$_2$ evolution rate, whereas the decrease of current efficiency with increasing electrolysis time may be due to the increase in the decomposition

amount of solid ferrate(VI) and/or the gradual passivation of iron wire anode. It should be noticed that the decreasing trend of purity with increasing electrolysis time may be proof of the increase in the decomposition ratio of solid ferrate(VI) with prolonged electrolysis time.

Figure 4 shows the influences of electrolysis current on apparent current efficiency, purity, and yield during the
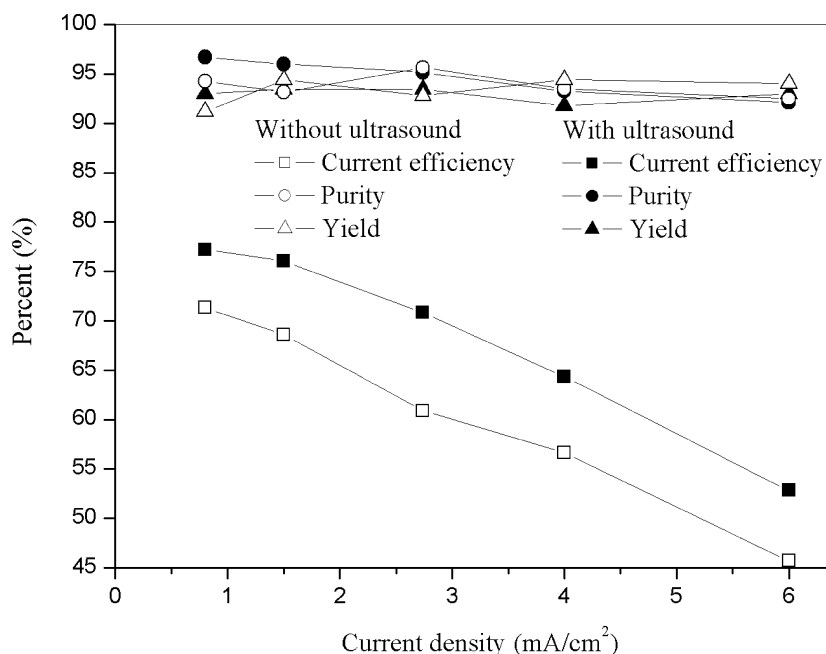

Fig. 4 Influence of electrolysis current on the apparent current efficiency, purity, and yield during the electrosynthesis of solid ferrate(VI) in 14 M KOH at 65 °C. Cell conditions are as described in Fig. 1 caption
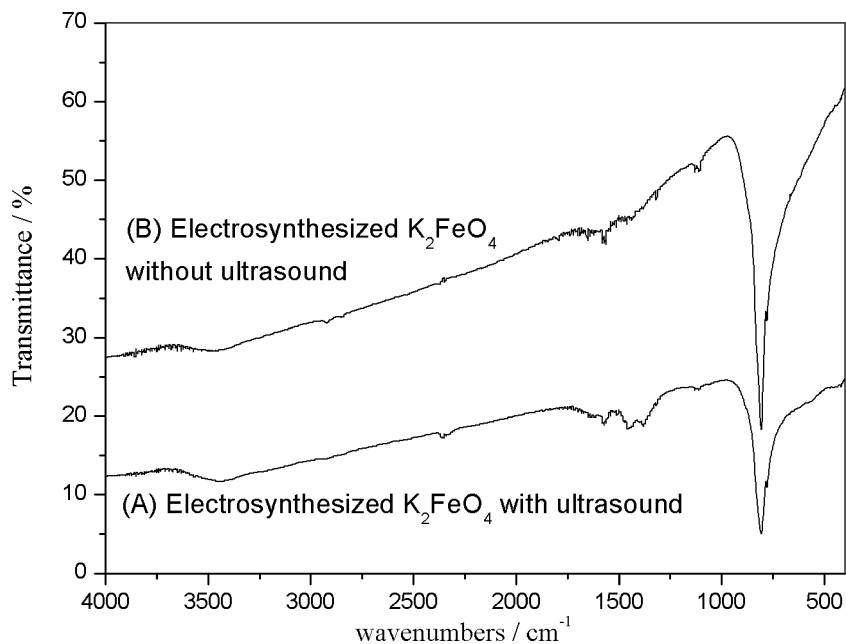
Fig. 5 FTIR spectra of solid K_2FeO_4 electrosynthesized **a** with ultrasound and **b** without ultrasound

electrosynthesis of solid ferrate(VI) in the absence and presence of ultrasound in 14 M KOH at 65 °C with a fixed charge of 3.0 A h (the sequential electrolysis time varying from 6.84 to 0.91 h). It can be found that, at various electrolysis currents, ultrasound obviously improves current efficiency, but it has less impact on the purity and yield of solid ferrate(VI). As the electrolytic current density increases, the passivation extent of the anode may be enhanced by the formation of surface layer, and the oxygen evolution rate is greatly increased. Meanwhile, more ferrate (VI) may be decomposed by the increase in the internal cell temperature resulting from the increase of the infrared (IR) heating rate [30]. This may result in the obvious decreasing trend of current efficiency with increasing electrolytic current density. As shown in Fig. 4, in the presence of ultrasound, the largest current efficiency 77.2% is obtained at the current density of 0.8 mA cm^{-2}, and the corresponding purity and yield are 96.7 and 93%, respectively.
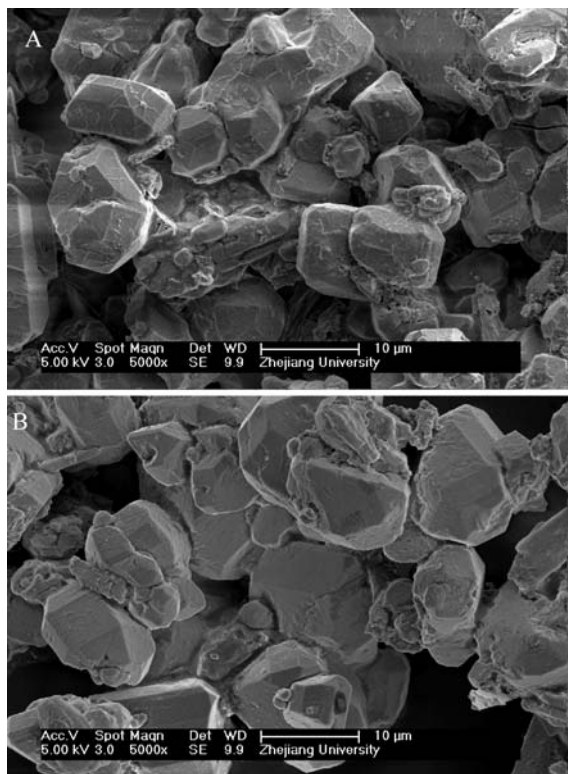

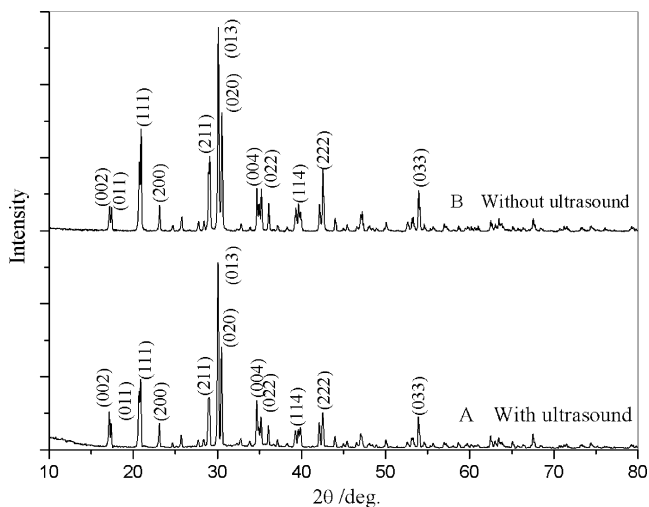**Fig. 6** SEM photos of solid K_2FeO_4 electrosynthesized **a** with ultrasound and **b** without ultrasound

Fig. 7 X-ray powder diffraction spectra of K_2FeO_4 electrosynthesized with and without ultrasound
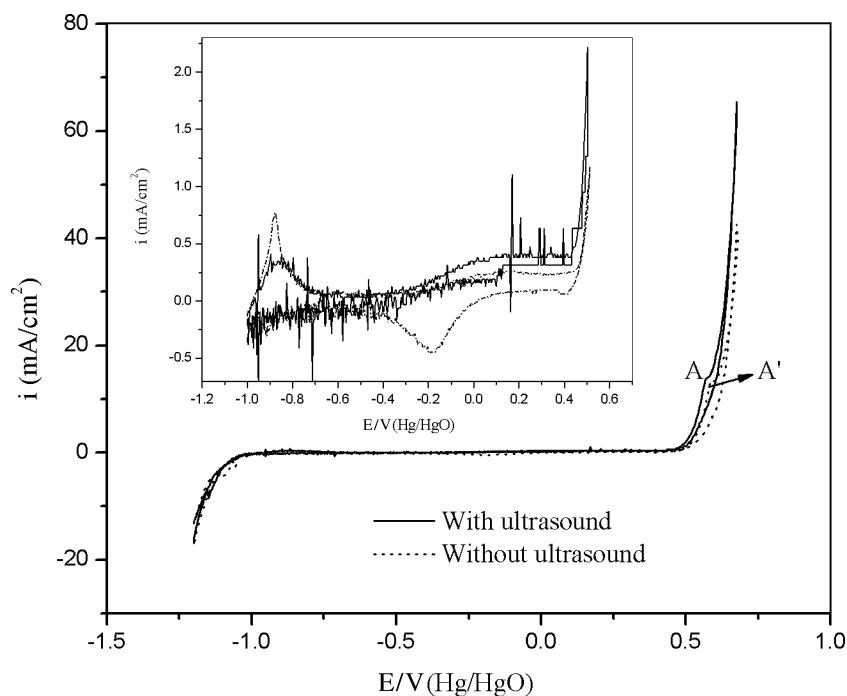
Fig. 8 Cyclic voltammetric curves of the pure iron electrode in 14 M KOH at 65 °C. The *inset* shows the magnification of the CV curve between −1.0 and 0.5 V; scan rate, 0.1 mV/s; ultrasonic power, 14.6 W

Figure 5 indicates that both the IR spectra with and without ultrasound are similar, possessing a strong absorption peak at 807 cm^{-1} and a shoulder peak at 781 cm^{-1}. The SEM photos in Fig. 6 show that both the solid ferrate(VI) samples manifest polyhedral shape and almost identical grain size. The XRD patterns in Fig. 7 indicate that both samples show the characteristics of K$_2$FeO$_4$ with an orthorhombic unit cell [31]. The above results show that the existence of ultrasound during electrosynthesis produces little impact on the physical properties of solid K$_2$FeO$_4$ samples.

Effects of ultrasound on the anodic behaviors of pure iron electrode

To further understand the effects of ultrasound on the direct electrosynthesis of solid K$_2$FeO$_4$, the anodic behaviors and surface structure of the planar electrode of pure iron were investigated.

The cyclic voltammetric (CV) curves of the pure iron electrode in 14 M KOH solution at 65 °C are illustrated in Fig. 8. The inset in Fig. 8 shows a magnification for the low current scale to present more information. The oxidation peaks at ca. −0.9 V represent the oxidation reactions of Fe to Fe(II) and/or Fe(III) [32, 33]. Larger passive current in the presence of ultrasound indicates that the passivation extent of the iron anode is decreased, which may result from the cavitation and microstreaming effects of ultrasound. In the transpassive region, the rapid increase of

current density with increasing electrode potential results from the formation of ferrate(VI) and oxygen evolution, and peaks A and A′ may represent the formation of ferrate (VI) [33]. It is noticed that the formation potential of ferrate (VI) in the presence of ultrasound is lower than that in the absence of ultrasound, which indicates that ultrasound can improve the electrosynthesis of ferrate(VI). The cathodic current peak at ca. −0.18 V on the cyclic voltammetric curves without ultrasound may be attributed to the reduction of solid ferrate(VI) on the electrode surface. However, the cathodic peak representing the reduction of solid ferrate(VI) can hardly be found on the curve in the presence of ultrasound, which may imply that ultrasonic stirring helps to expel out the solid ferrate(VI) adsorbed on the electrode surface to the bulk electrolyte. This may be the reason why the passivation extent of iron anode is decreased in the presence of ultrasound.

Moreover, for the 2 h electrolysis with the constant current of 0.81 mA at 65 °C in 14 M KOH solution, the collected amount of O$_2$ evolution for the pure iron anode in the presence of ultrasound is 0.112 ml, while the amount in the absence of ultrasound is 0.166 ml. This indicates that ultrasound can decrease the O$_2$ evolution rate on the pure iron, which also implies that the current efficiency for the electrosynthesis of ferrate(VI) can be improved in the presence of ultrasound.

The morphologies of pure iron electrode with and without ultrasound after 2 h electrolysis in 14 M KOH at 65 °C are illustrated in Fig. 9. It can be seen that the surface

Fig. 9 SEM photos of pure iron surface without (**a** and **b**) and with (**c** and **d**) ultrasound. Ultrasonic power, 14.6 W
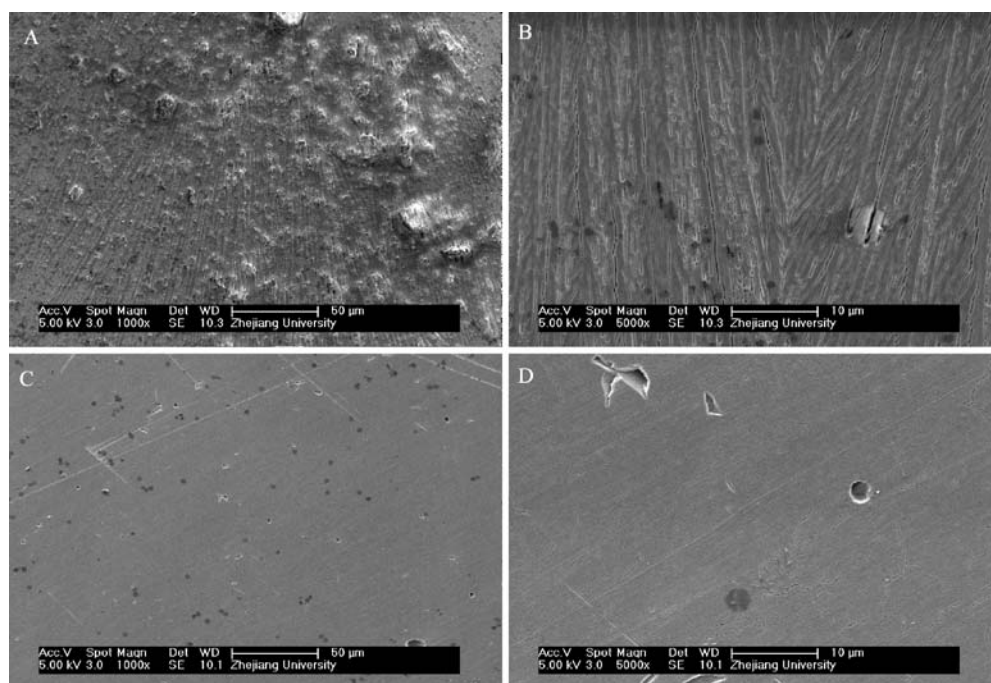
of iron anode is covered with intermediate iron oxide and/or some ferrate(VI) products in the absence of ultrasound, while the iron anode has much less surface product or oxide layer in the presence of ultrasound. This is in good agreement with the CV results. It is also noted in Fig. 9 that some tiny openings occur on the surface of iron anode, which indicates that the solid ferrate(VI) may be electrosynthesized through the local dissolution of iron anode on the active sites.

Conclusions

The electrosynthesis of solid ferrate(VI) at 65 °C in 14 M KOH displays much higher current efficiency in the presence of ultrasound, and this may result from lower formation potential of ferrate(VI), less passivation extent of iron anode, and lower O_2 evolution rate caused by the existence of ultrasound.

In the power range from 14.6 to 35.6 W, the decomposition rate of solid ferrate(VI) increases with the increase of ultrasonic power, which results in the slight decrease of apparent current efficiency with increasing ultrasonic power.

It is found that, in the scope of our experiments, shorter electrolysis duration and smaller electrolysis current are advantageous to improve the direct electrosynthesis of solid ferrate(VI) in terms of current efficiency and that ultrasound produces little impact on the physical properties of solid K_2FeO_4 samples

References

1. Sharma VK (2002) Adv Environ Res 6:143
2. Delaude L, Laszlo P (1996) J Org Chem 61:6360
3. Licht S, Wang BH, Ghosh S (1999) Science 285:1039
4. Licht S, Wang BH, Xu G, Li J, Naschitz V (1999) Electrochem Commun 1:527
5. Yang WH, Wang JM, Pan T, Xu JJ, Zhang JQ, Cao CN (2002) Electrochem Commun 4:710
6. Licht S, Tel-Vered R, Halperin L (2004) J Electrochem Soc 151:A31
7. Licht S, Tel-Vered R (2004) Chem Commun 628
8. Licht S, Naschitz V, Ghosh S (2002) J Phys Chem B 106:5947
9. Licht S, Naschitz V, Rozen D, Halperin N (2004) J Electrochem Soc 151:A1147
10. Bouzek K, Schmidt MJ, Wragg AA (1999) Electrochem Commun 1:370
11. Bouzek K, Lipovska M, Schmidt MJ (1998) Electrochim Acta 44:547
12. Bouzek K, Schmidt MJ, Wragg AA (1999) J Chem Technol Biotechnol 74:1188
13. Lapicque F, Valentin G (2002) Electrochem Commun 4:764
14. Denvir A, Pletcher D (1996) J Appl Electrochem 26:815
15. Koninck MD, Belanger D (2003) Electrochim Acta 48:1435
16. He WC, Wang JM, Shao HB, Zhang JQ, Cao CN (2005) Electrochem Commun 7:607
17. Jiang JQ, Lloyd B (2002) Water Res 36:1397
18. Kowalska E, Mizera J (1971) Ultrasonics 9(2):81
19. Alkire RC, Stephen P (1983) Corros Sci 23(10):1121
20. Perusich SA, Alkire RC (1991) J Electrochem Soc 138(3):708
21. Walton DJ, Phull SS (1996) In: Mason TJ (ed) Advances in sonochemistry, vol 4. Elsevier, p 205

22. Doche ML, Hihn JY, Touyeras F, Lorimer JP, Mason TJ, Plattes M (2001) Ultrason Sonochem 8:219
23. Sáez V, García JG, Iniesta J, Ferrer AF, Aldaz A (2004) Electrochem Commun 6:757
24. Walton DJ, Phull SS, Geissler U, Chyla A, Durham A, Ryley S, Mason TJ, Lorimer JP (2000) Electrochem Commun 2:431
25. Doche ML, Hihn JY, Mandroyan X, Viennet R, Touyeras F (2003) Ultrason Sonochem 10:357
26. Schreyer JM, Thompson GW, Ockerman LT (1950) Anal Chem 22:1426
27. Mason TJ, Lorimer JP, Bates DM (1992) Ultrasonics 30:40
28. Contamine RF, Wilhelm AM, Berlan J, Delmas H (1995) Ultrason Sonochem 2(1):S43
29. Compton RG, Eklund JC, Marken F (1997) Electroanalysis 9 (7):509
30. Licht S, Tel-Vered R, Halperin L (2002) Electrochem Commun 4:933
31. Audette RJ, Quail JW, Black WH, Robertson BE (1973) J Solid State Chem 8:43
32. Beck F, Kaus R, Oberst M (1985) Electrochim Acta 30:173
33. Bouzek K, Raušar I, Bergmann H, Hertwig K (1997) J Electroanal Chem 425:125